

Modeling active sensing reveals echo detection even in large groups of bats

Thejasvi Beleyur^{a,1} and Holger R. Goerlitz^{a,1}

^aAcoustic and Functional Ecology, Max Planck Institute for Ornithology, 82319 Seewiesen, Germany

Edited by Terrence J. Sejnowski, Salk Institute for Biological Studies, La Jolla, CA, and approved November 3, 2019 (received for review December 20, 2018)

Active sensing animals perceive their surroundings by emitting probes of energy and analyzing how the environment modulates these probes. However, the probes of conspecifics can jam active sensing, which should cause problems for groups of active sensing animals. This problem was termed the cocktail party nightmare for echolocating bats: as bats listen for the faint returning echoes of their loud calls, these echoes will be masked by the loud calls of other close-by bats. Despite this problem, many bats echolocate in groups and roost socially. Here, we present a biologically parametrized framework to quantify echo detection in groups. Incorporating properties of echolocation, psychoacoustics, acoustics, and group flight, we quantify how well bats flying in groups can detect each other despite jamming. A focal bat in the center of a group can detect neighbors in group sizes of up to 100 bats. With increasing group size, fewer and only the closest and frontal neighbors are detected. Neighbor detection is improved by longer call intervals, shorter call durations, denser groups, and more variable flight and sonar beam directions. Our results provide a quantification of the sensory input of echolocating bats in collective group flight, such as mating swarms or emergences. Our results further generate predictions on the sensory strategies bats may use to reduce jamming in the cocktail party nightmare. Lastly, we suggest that the spatially limited sensory field of echolocators leads to limited interactions within a group, so that collective behavior is achieved by following only nearest neighbors.

active sensing | bioacoustics | group behavior | psychoacoustics | sonar interference

Active sensing animals use self-generated energy to sense their surroundings by analyzing how objects around them change the emitted energy (1). Bats emit loud ultrasonic calls and detect objects around them by listening to the echoes (2, 3) reflected off these objects. Active sensing is an effective sensory modality when the animal is solitary. However, when multiple active sensing animals emit pulses of energy in close proximity, they may “jam” each other and mutually interfere with their ability to detect objects in their environment (1, 4). If groups of echolocating bats mutually jam or mask each other, they would not be able to detect each other. Due to the intense jamming, individuals would have a progressively difficult time detecting the echoes reflecting off their neighbors, and thus not detect their neighbors at all. Without detecting each other, groups of individuals cannot show collision-free flight. However, many bat species are very gregarious, and fly and echolocate together in groups of tens to millions of bats. Bat groups also show coordinated behaviors in cave flights, evening emergences, and mating swarms (5, 6). How is their ability to detect each other impaired by increasing group size? How many of its neighbors does a bat actually detect in the presence of intense jamming? What strategies may improve echo detection and thus neighbor detection when many active sensing animals are together? We present biologically parametrized simulations to answer how bats manage to echolocate in the face of intense jamming.

In human psychophysics, the sensory challenge of perceiving an auditory cue among other similar sounds has been called the “cocktail party problem” (7, 8). When applied to bat echolocation,

the cocktail party problem has been elevated to the “cocktail party nightmare,” given the high repetition rate, similarity, and amplitude of echolocation calls. On top of these factors is the nonlinear increase in the number of masking sounds with increasing group size (9). Empirical studies to date have investigated the cocktail party problem from a sender’s perspective (7, 9, 10). Through field observations, playback studies, and on-body tags (11–22), we now know a range of echolocation strategies that bats show under challenging acoustic conditions. Bats can increase their call intensity, alter their call duration and frequency range, or suppress calling in the presence of conspecifics and noise playbacks (11, 20, 23, 24). In contrast to the many reports of bats’ responses to noisy conditions, very little work has been done in conceptually understanding how receiver strategies might contribute to dealing with the cocktail party nightmare (25, 26). To our knowledge, biological modeling of the cocktail party nightmare from a receiver’s perspective that includes the details of bat echolocation and auditory processing is lacking. We fill this gap in conceptual understanding by presenting a biologically parametrized model based on the known properties of bat audition and the acoustics of a multibat echolocation scenario. We quantified how well a bat flying with conspecifics can perceive its neighbors in terms of the returning echoes it detects. Through our simulations, we arrive at a sensory estimate of what a bat in the cocktail party nightmare may be detecting, if anything at all.

Significance

Close-by active sensing animals may interfere with each other. We investigated what echolocators flying in a group hear—can they detect each other after all? We modeled perceptual and acoustic properties in group echolocation to quantify neighbor detection probability as group size increases. Echolocating bats can detect at least 1 of their closest neighbors per call up to group sizes of even 100 bats. Call parameters such as call rate and call duration also play a strong role in how much echolocators in a group interfere with each other. Even when many bats fly together, they are indeed able to detect at least their nearest frontal neighbors—and this prevents them from colliding into one another.

Author contributions: T.B. and H.R.G. designed research; T.B. performed research; T.B. analyzed data; and T.B. and H.R.G. wrote the paper.

The authors declare no competing interest.

This article is a PNAS Direct Submission.

Published under the PNAS license.

Data deposition: All code required to replicate the simulations, results, analyses, and figures in this paper are available at this Zenodo repository link: <https://doi.org/10.5281/zenodo.3529691>. All raw data and code required to replicate the results of the experimental parametrizations (target strength and acoustic shadowing) are available at the following repository link: <https://doi.org/10.5281/zenodo.3469845>.

¹To whom correspondence may be addressed. Email: thejasvib@gmail.com or hgoerlitz@orn.mpg.de.

This article contains supporting information online at <https://www.pnas.org/lookup/suppl/doi:10.1073/pnas.1821722116/-DCSupplemental>.

Material and Methods

We model the echolocation of frequency-modulating (FM) bats. The calls of FM bats are typically downward frequency-modulated and of short duration (≤ 5 ms). Each call is followed by a longer silence (80–150 ms) called the interpulse interval (27). FM bats thus sense their world “stroboscopically” by emitting a call and listening for the echoes returning during the interpulse interval (28). In the absence of any loud conspecific calls, a bat is able to hear all returning echoes and thus to detect all objects around it. However, in the presence of other loud bat calls, some of its own returning echoes may be masked. In that case, the bat will hear a few or none of the returning echoes. This corresponds to the bat detecting a few or none of the surrounding objects. In the cocktail party nightmare the “objects” each bat is trying to detect are its neighbors.

Our model of the cocktail party nightmare is designed to describe the auditory scene (9) of a bat emerging from a cave in a group as it echolocates on the wing. A focal bat flying in a group of N bats may detect up to $N-1$ of its neighbors (excluding itself), which is equivalent to hearing $N-1$ returning echoes. The focal bat receives 2 kinds of loud masking sounds that interfere with the detection of its neighbors: 1) the $N-1$ loud calls emitted by other bats in the group, and 2) the secondary echoes created by the call of a neighboring bat, reflecting once off another bat, and arriving at the focal bat. Every neighboring bat call generates $N-2$ secondary echoes, meaning that the focal bat can receive up to $N-1 \times N-2$ secondary echoes (Fig. 1). We implemented a spatially explicit 2-dimensional (2D) simulation of bat echolocation, sound propagation, and sound reception and include mammalian auditory phenomena to quantify how many and which neighbors a bat can detect in the sonar cocktail party nightmare. We then explored how changes in group size and in sender strategies affect neighbor detection in a group.

Model Scenarios. We ran 2 model scenarios to test the effect of 1) increasing group size and of 2) variation in call parameters, group geometry, and acoustic parameters on neighbor detection. In all models, we used the central-most bat in the group as the focal bat.

Scenario 1: Effect of group size on neighbor detection. We simulated groups of 5, 10, 30, 50, 75, 100, and 200 well-aligned bats with identical echolocation and hearing properties flying at a minimum interbat distance of 0.5 m (Table 1 for full model parameters). The number and location of neighbors detected by the focal bat were recorded in every simulation run.

Scenario 2: Effect of call parameters, group geometry, and acoustic parameters on neighbor detection. Here, we varied other parameters relevant to the cocktail party nightmare (Table 1) while keeping group size constant ($n = 100$, i.e., the largest group size from Scenario 1 with a biologically relevant neighbor detection rate). We varied call parameters (interpulse interval, call duration, source level), group parameters (heading variation, minimum interbat spacing), and acoustic parameters (atmospheric absorption, acoustic shadowing).

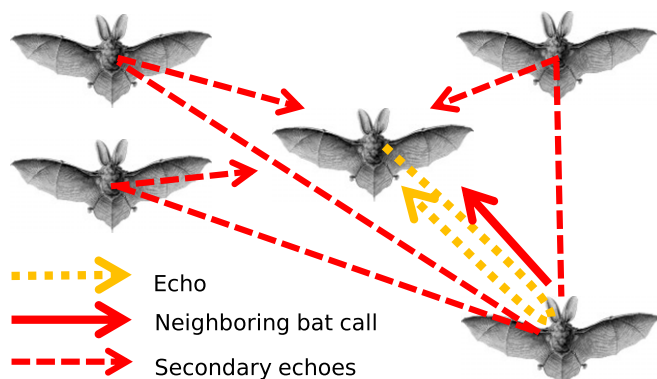


Fig. 1. Schematic of the cocktail party nightmare. Arrows indicate the different types of sounds received by a focal bat: it needs to hear the echoes returning from its own calls (orange) to detect its neighbors, despite the masking by the calls of neighboring bats (solid red) and their secondary echoes (dashed red). Here, only 1 target echo off a single neighbor, only 1 representative neighboring bat call, and its set of secondary echoes are shown. In total, for a group of N bats, the focal bat will receive $N-1$ echoes, $N-1$ neighboring bat calls, and $N-1 \times N-2$ secondary echoes. Bat image courtesy of Wikimedia Commons/Ernst Haeckel.

Model Implementation. Each model run simulated 1 interpulse interval of the focal bat, and we calculated the timing and received level of all sounds (target echoes, masking calls, and secondary echoes) that arrived at the focal bat during that interpulse interval. Each model run simulated a series of sounds that arrived during an interpulse interval following the focal bat's call, based on a spatially explicit distribution of a group of bats (*SI Appendix, Schematic S1*). At the beginning of every model run, N bats were placed in a 2D space with randomly assigned heading directions (*SI Appendix, sections 1.6 and 1.7*). For each neighboring bat, we calculated its angle and distance to the focal bat. The received level was calculated based on a common source level for all bats, spherical and atmospheric spreading over each call's and echo's travel distance, and acoustic shadowing. Acoustic shadowing is the reduction in received level of a sound due to obstructions in its path. A sound in the cocktail party nightmare may pass around obstacles (other bats) as it propagates from source to receiver. The reduction in received level was measured and calculated as a linear function of the number of bats obstructing the path between source and receiver (*SI Appendix, section 1.9*). For target and secondary echoes, we also considered monostatic and bistatic target strengths measured in this paper (*SI Appendix, section 1.8*).

The arrival time of target echoes within the interpulse interval was determined according to the 2-way travel time to the echo-reflecting neighboring bat. The arrival time of masking calls and secondary echoes was assigned randomly with uniform probability across the interpulse interval. The random arrival time assignment of calls and secondary echoes recreates the uncoordinated echolocation of all bats in the group. It is unlikely that multiple bats in large groups can coordinate their calls effectively, and independent calling has been reported even in small groups of 4 bats (29).

All bats in a group were identical in their calling properties, and we treated all sounds as constant tones of equal duration, i.e., we did not explicitly model spectral emission, propagation, and reception properties. The only difference between each of the sounds was their path and source of sound production. The omission of spectral properties is a conservative choice that assumes maximal masking of the primary echoes, thus allowing us to study the role of intensity differences and temporal separation between target echoes and masking sounds.

Once we calculated the timing and received level of all sounds at the focal bat, we accounted for directional hearing sensitivity (*SI Appendix, Fig. S3*) and spatial unmasking. Spatial unmasking describes the reduction in experienced masking as the arrival angle between masker and target sound increases (30, 31). We simulated spatial unmasking by the reduction of a masker's effective received level based on its angular separation to an echo. For each echo, the same masker will have a different effective masking level as its relative angle of arrival will be unique for each echo. We thus calculated the effective masking level of each masker for each echo. The effective masking levels of all maskers were then combined to form a time-variant and echo-specific “masker SPL profile” (*SI Appendix, Fig. S5D*). This is essentially the joint sound pressure level (SPL) of all maskers over time. We then expressed this echo-specific masker SPL profile in relation to the echo's SPL, thus obtaining a relative “echo-to-masker ratio profile” (*SI Appendix, Fig. S5E*). This is equivalent to a signal-to-noise ratio profile, where the echo is the signal and the masker profile is the noise.

In addition to angular separation, signal detection is also determined by the temporal separation between signal (echo) and masker (24, 32, 33). Masking increases as the masker arrives closer in time to the echo. Masking occurs over longer durations when maskers arrive before the signal (forward masking) than afterward (backward masking). We recreated the asymmetric masking by a “temporal masking envelope” temporally centered at the echo (*SI Appendix, Fig. S1*). The echo was considered heard if the echo-to-masker ratio profile was above the temporal masking envelope. We allowed short drops of the echo-to-masker ratio profile below the temporal masking envelope, for a combined maximum duration of less than 25% of an echo's duration. Alternatively, we defined an echo to be masked (= not heard), if the echo-to-masker ratio profile was below the temporal masking envelope for more than 25% of the echo duration. The 25% threshold was an arbitrarily chosen conservative value to prevent masking by rare and short bursts of high sound pressure level that are unlikely to affect echo detection biologically (*SI Appendix, section 2.7*).

Model Parametrization. We implemented a detailed set of echolocation, group and sound properties in our model, including call and hearing directionality, spatial unmasking, temporal masking, group geometry, and details of sound propagation. These properties were parameterized based on published results wherever available. Acoustic shadowing and target strengths (monostatic and bistatic) of bats were specifically measured for this work. All details of the model parameters including our respective measurements and on model implementation are presented in the Supporting Information.

Table 1. Model parameters for both model scenarios

Parameter	Scenario 1: Effect of group size	Scenario 2: Effect of call parameters, group geometry, and acoustics
Group size	5, 10, 30, 50, 75, 100, 200	100
Interpulse interval (ms)	100	25, 50, 100, 200, 300
Call duration (ms)	2.5	1, 2.5
Source level (dB SPL re 20 μ Pa at 1m)	100	94, 100, 106, 112, 120
Minimum interneighbor distance (m)	0.5	0.5, 1.0
Group heading variation ($^{\circ}$)	10	10, 90
Atmospheric attenuation (dB/m)	-1	0, -1, -2
Acoustic shadowing	Yes	No, Yes

Scenario 1 modeled the effect of group size, while other parameters were fixed, resulting in 7 parameter combinations (1 per group size). Scenario 2 modeled the effect of other relevant parameters, while group size was kept constant at 100 bats, resulting in a combined set of 1,200 parameter combinations.

Results

Effect of Group Size on Neighbor Detection. At group sizes of 5 and 10, the focal bat hears the echoes of most or all of its neighbors per call (median: 4 and 8 echoes per call at $n = 5$ and 10, respectively; Fig. 2). At progressively larger group sizes, the median number of detected neighbors drops from 4 to 0 at group sizes of 30 to 200. Yet even in a group of 100 bats, while the median number of detected neighbors is zero, the 90th percentile is 1, showing that a neighbor is not detected with each call, but occasionally. Beyond a group of 100 bats, the focal bat typically detects no neighbors at all. The initial rise in detected neighbors in groups of 5 to 30 bats is primarily caused by the increased number of neighbors that could be detected, which is soon counteracted by the intense masking that rises nonlinearly with group size.

We next derived the probability of detecting at least 1 neighbor per call, which describes the average rate of neighbor detection (Fig. 3A, blue). At smaller groups of 5 to 30 bats, the focal bat detects at least 1 neighbor per call at above 0.95 probability. At larger group sizes (50 to 100), the probability of detecting at least 1 neighbor drops rapidly to 0.3 per call in a group of 100 bats, and is basically zero for a group of 200 bats (0.004 probability). A bat (with 10 Hz calling rate) flying in a group of 100 bats will thus detect at least 1 neighbor around 3 times per second (~ 3 Hz detection rate), while a bat flying in a group of 30 bats will detect at least 1 neighbor almost every time it calls (9.5 Hz detection rate). The probability of detecting multiple bats per call is lower than just detecting at least 1 bat (Fig. 3A). Yet, even in a group of 50 bats, the focal bat has a probability of detecting at least 2 and 4 neighbors per call of about 0.5 and 0.1, respectively.

We next quantified which neighbors the focal bat detects. Detection is generally limited to nearby neighbors (Fig. 3B) and, with increasing group size, to neighbors in front of the focal bat (Fig. 3C). At a group size of 30 bats, the focal bat occasionally detects neighbors that are up to 2 m away in radial distance, which is the furthest neighbor distance. With increasing group sizes, despite the group being more spread out, the focal bat can only detect its nearest neighbors (e.g., neighbors at ~ 0.5 m in a group of 200 bats; Fig. 3B). In the azimuthal plane, at small group sizes, the focal bat initially detects neighbors all around it (95%-neighbor detection angle range $\geq 237^{\circ}$ for up to 50 bats; Fig. 3C). With increasing group size, a frontal bias in neighbor detection appears (95%-neighbor detection angle range: 191 to 35° for 100 and 200 bats; Fig. 3C).

Effect of Call Parameters, Group Geometry, and Acoustic Parameters on Neighbor Detection. We next analyzed how variation in call parameters, group structure, and acoustic parameters affected neighbor detection. We fixed the group size to 100, as at this size, the focal bat could typically detect at most 1 neighbor (90th percentile, Fig. 2) at 0.3 probability (Fig. 3A) per call. We thus reduced the output of each simulation run to a binary neighbor detection score of 1 (detection) or 0 (no detection). We analyzed the effect of each parameter on neighbor detection with a logistic regression,

treating all parameters as categorical and using their value in Scenario 1 as reference (parameter range in Table 1).

The call parameters interpulse interval and call duration showed the strongest effect (Fig. 4A and B and *SI Appendix, Table S2*). Increasing the interpulse interval from 100 ms to 200 and 300 ms increases neighbor detection probability by about 15 and 75 times, while reducing it to 50 ms lowers neighbor detection to 0.05 times (Fig. 4A). Shortening call duration from 2.5 ms to 1 ms led to 35 times higher neighbor detection (Fig. 4B). Call source level had no effect (Fig. 4C).

Group geometry also influenced neighbor detection probability, but less than changing call parameters. Flying at larger interbat distances of 1.0 m leads to 0.31 times lower neighbor detection compared to denser groups with 0.5 m interbat distance (Fig. 4D). Groups where individuals head in a more variable direction have 1.32 times better neighbor detection than groups with a generally common heading (or echolocation beam) direction (Fig. 4E).

Among the physical parameters, acoustic shadowing increased neighbor detection (without acoustic shadowing, neighbor detection is 0.75 times lower than with acoustic shadowing), while atmospheric attenuation had a negligible effect (Fig. 4F and G).

Discussion

We present a conceptual framework to quantify what a focal bat experiences in the sonar cocktail party nightmare. We quantified the probability of detecting neighbors across a range of group sizes, which allows calculating the rate at which a focal bat detects its neighbors. When flying alone, a focal bat will detect objects around it at a rate equal to its call rate, while in a group,

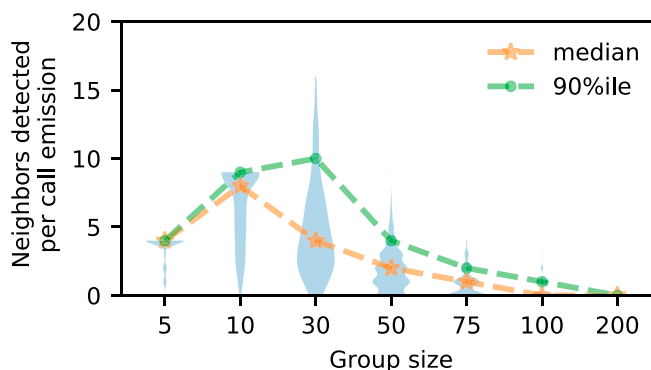


Fig. 2. Number of detected neighbors per call by a focal bat in the center of a group. The initial rise in the number of detected neighbors is because there are indeed more neighbors and the degree of masking is low. However, with increasing group size, most of the neighbors cannot be detected anymore, and progressively fewer neighbors are detected per call. Violin plots show the distribution of the number of neighbors detected per call, and their median (stars, orange) and 90th percentile (dots, green).

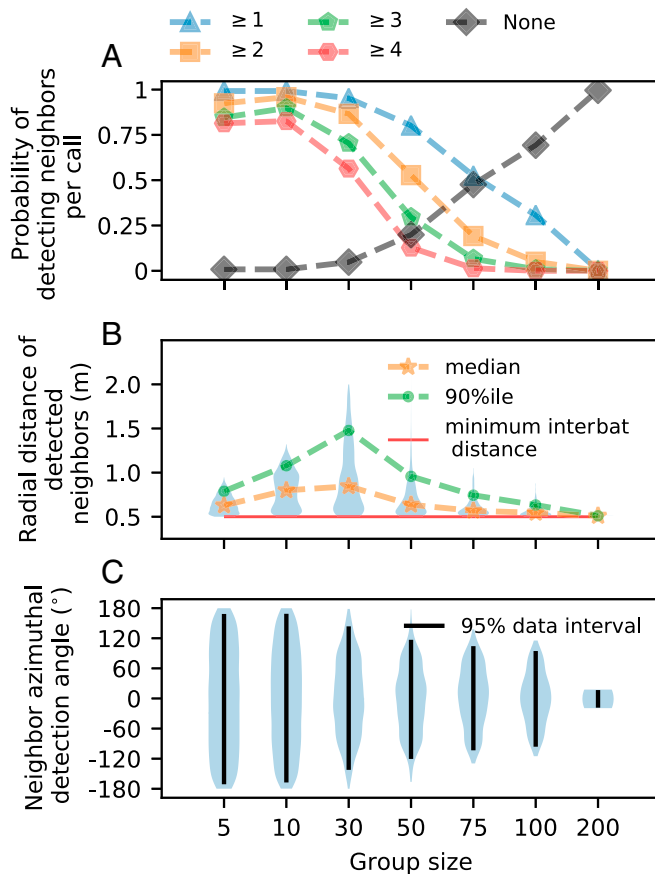


Fig. 3. Characterization of the focal bat's perception. (A) The probability of detecting $\geq X$ neighbors per call ($X = 1, 2, 3, 4$, or none). Even in groups of up to 100 bats, the focal bat has a ~ 0.3 probability of detecting at least 1 neighbor per call. In even larger groups (200 bats), no neighbors are detected anymore. (B) With increasing group size, a focal bat only detects its closest neighbors. Initially, the radial distance of detected neighbors increases because the spatial extent of a group increases with group size (at 5, 10, 30 bats: radius = 0.75, 1.12, 1.97 m), but it then drops down to the nearest neighbors beyond 30 bats. (C) The azimuthal location of detected neighbors, showing an increasing frontal bias with increasing group size. Although neighbors were uniformly distributed in azimuth, the frontal bias of call and hearing directionality means that frontal returning echoes are louder than peripheral ones.

its object detection rate is reduced due to masking. We show that even in a group of 100 bats, bats still detect at least 1 neighbor per call about 3 times per second (for a 10 Hz call rate), while in smaller group sizes, neighbor detection rate is larger at 5 to 10 Hz. Bat echolocation is generally “stroboscopic,” meaning that information is received intermittently with time gaps (3). We suggest that bats in smaller group sizes still experience a sufficiently high information update rate for performing collision avoidance and neighbor following. With increasing group size, perception might become “hyper-stroboscopic,” i.e., so scarce that different sensorimotor heuristics might be required to maintain group coordination.

The low level of masking at smaller group sizes allows the focal bat to detect all its neighbors per call. With increasing group size, however, the focal bat detects maximally 1 neighbor per call in a group of 100 bats. This neighbor detection rate of at least 1 neighbor per call even in large group sizes provides a formal sensory basis for group movement in active sensing animals. While a bat in a large group cannot track the position of all its neighbors, it still can track the movement of a few neighbors, specifically those close to and in front of it. This reduction in rate, range, and direction of

detected neighbors has predictive consequences for the kind of collective behavior bat groups may show in nature. Many models of collective movement assume that each individual in a group detects the position and orientation of neighbors in the whole of its sensory volume, and then performs an averaging across all neighbors to decide its next movement (34–37), leading to the impressive coordinated behaviors of fish schools and insect swarms (38, 39). As the number of neighbors that an individual detects decreases, more “limited interactions” begin to dominate, causing anisotropy in the group structure (40, 41). For bats in the cocktail party nightmare, we predict that large groups may show higher anisotropy than smaller groups due to the limited number of neighbors that they can detect and react to. All things being equal, we predict that in large groups (>50 bats), the neighbors in the frontal field of a bat will have a disproportionate influence on its movement decisions. Bats in larger groups may thus maintain higher alignment with their frontal neighbors compared to bats in smaller groups.

Our simulations allow for a direct quantitative comparison of the effects of echolocation, group geometry, and acoustic parameters in group echolocation. Among the call parameters tested, reducing call rate (increasing interpulse interval) was most effective in increasing neighbor detection in jamming conditions, matching experimental evidence for reduced calling rate in *Tadarida brasiliensis* (19, 20). In contrast, other FM bat species increase their call rates in groups and background noise (11, 15, 42, 43). Likewise, our result that shorter call duration should improve neighbor detection is opposite to experiments showing that most bat species increased call duration in the presence of maskers (11, 23, 24, 43, 44), except (42). Lastly, our result of no effect of changing source level on neighbor detection might also seem to differ from experimental data showing that bats in laboratory conditions do increase source level in the presence of maskers (11, 23, 43, 44). While there might be species-specific variation, we suggest that these differences are mostly due to the experimental situation. Bats in these experiments experienced constant maskers. Calling more often, for longer, and for louder thus improved the bats' signal redundancy, echo-to-masker ratio, and overall echo detection. In contrast, our model simulates group flight of many bats with simultaneous and uniform changes in their call parameters. When all bats in a group shorten call duration, this reduces the overall duration of masking sounds, thus improving echo detection. Likewise, when all bats in a group increase their call amplitudes to optimize their own echo-to-masker ratios, all bats will eventually call at their maximum, with no overall effect on neighbor detection. Analyzing bat calls in mass emergences is technically challenging and it remains unknown whether *T. brasiliensis* and other gregarious bat species reduce their call rate in the field.

Bat aggregations show a variety of structures across behavioral contexts, from well-aligned almost parallel flight during roost emergences, to more variable and less-aligned flight in mating swarms and when circling in limited cave volumes. We show that this group structure itself affects how well bats can detect each other. Bats detect their neighbors better in less-aligned groups compared to more aligned groups. During aligned emergence flight, the focal bat always receives loud forward-directed masking calls from bats behind it, in addition to the relatively loud side-calls emitted by neighbors to its left and right. In contrast, during less-aligned swarming flight, the relative orientation of the bats is more distributed and changing, with the focal bat experiencing a wider dynamic range of masker levels (i.e., louder and fainter masking calls originating from a wider range of angular directions). This increased dynamic masker range allows for better echo detection, as there will be drops in echo-to-masker ratios due to changing received masker level. This effect is beneficial for enabling swarming flight, as the collision risk in less-aligned flight is likely higher compared to the more aligned emergence flight.

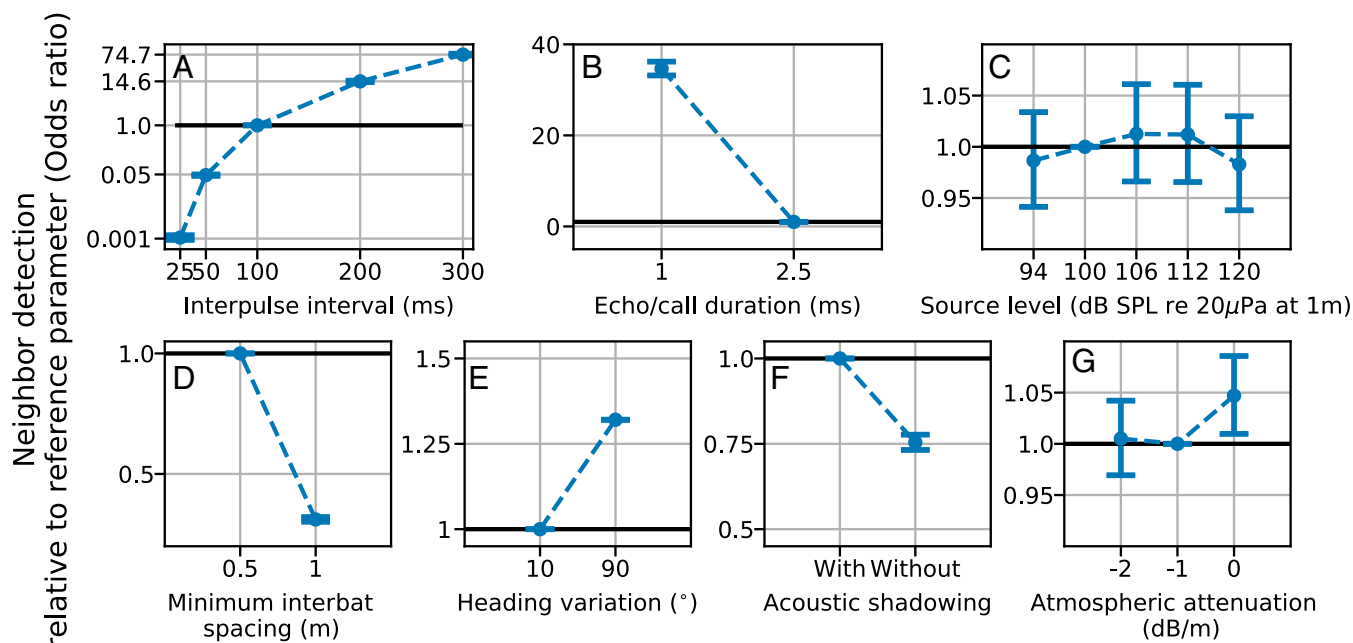


Fig. 4. Effect of call parameters (A–C), group geometry (D and E), and acoustic parameters (F and G) on neighbor detection. Each plot shows the probability of neighbor detection (model estimate and 95% confidence interval of odds ratio) when changing model parameters relative to the reference parameter used in the simulations of Scenario 1 (Table 1). Odds ratios above and below 1 indicate a higher and lower neighbor detection probability, respectively, indicated by the horizontal reference line. (A–C) Call parameters: Longer interpulse intervals (A) and shorter call durations (B) increase neighbor detection probability, while call source level (C) has no effect. (D and E) Group geometry: Neighbor detection is better in groups that are tightly packed (D) and with higher heading variation (E). (F and G) Effect of acoustic parameters: Acoustic shadowing by bats in groups improves neighbor detection probability (F), while atmospheric attenuation has a negligible effect (G).

Interindividual distance is another parameter of group structure, and we show that neighbor detection is better in dense groups. This might seem unexpected given that the received SPL of the maskers is higher the closer the bats are to each other. However, received echo levels are also higher when bats are closely spaced. Since echo SPL drops by 12 dB per doubling of distance, but masker call SPL only by 6 dB per doubling of distance, the echo-to-masker ratio is higher at shorter compared to longer interbat distances. It would be interesting to examine if perhaps large groups in the field actually fly closer to each other than smaller groups.

While we only modeled neighbor detection for the central-most bat in a group, its position in the group (e.g., central, frontal, or at the back) is likely to also have an effect on the number and received level of maskers, and thus on the number of detected echoes. However, we expect the obtained trends to remain qualitatively the same regardless of focal bat position. Particularly, we predict that masking will increase with group size, and only the exact group size at which a given level of masking (e.g., X% neighbor detection probability) is obtained will change depending on the focal bat's position in the group.

We furthermore show that it is important to consider bats not only as sources of reflected echoes and masking sounds, but also as obstructions to sound that actually alleviate the cocktail party nightmare. Typically, the detected echoes originate from nearby bats and are not shadowed. In contrast, the masking calls and secondary echoes can arrive from distant neighbors, thus passing by multiple other bats. Shadowing thus consists of the overall reduction in masker levels, which increases echo-to-masker ratios for the comparatively loud echoes returning from nearby neighbors.

Our results show that the cocktail party may not be as much of a “nightmare” as previously thought (9). We show that the modeled psychoacoustic, spatial, and acoustic properties act together to alleviate the nightmare into a challenge. When bats are flying in a multiecho environment, our results show that a bat will

always hear some echoes after a call emission, and very rarely no echoes at all. This parallels the phenomenon of auditory “glimpsing” reported in the human auditory cocktail party where individuals may follow conversations by perceiving parts of detected speech rather than whole sounds (45).

Improved Echo Detection in Real-World Situations. We present a first approximation to the sonar cocktail party nightmare, including many relevant biological, physical, and auditory mechanisms. Bats are expert echolocators and can detect echoes and fly under challenging conditions (24, 46–48). Bats rapidly adjust their call behavior in terms of their call duration, source level, and interpulse intervals (49, 50), integrate echoic information over multiple call emissions (51), and actively track objects by aiming their calls at them (52, 53). While we tested a range of different echolocation call parameters, our model implemented these parameters as fixed values that do not vary over time, thus lacking the dynamic nature of a real bat in the wild.

Furthermore, we did not model the spectral content of echo or masker sounds, and analyzed echo detection based on a fixed threshold of echo-to-masker-ratio. In contrast, real echolocation calls possess a time-variant spectral pattern that is species and even individual specific (13, 54), which can reduce echo masking. Masking is strongest when target and masker overlap both in time and in frequency (i.e., fall within the same critical band of the auditory system) (32, 55). The frequency-modulation of bat calls means that even when maskers and echoes partially overlap in time, they will not necessarily overlap in frequency, thus reducing the likelihood of masking. The individuality of bat calls may help a bat reject the secondary echoes from other bats' calls by forming separate auditory streams (56) for its own echoes and others' echoes. Given the scarcity of empirical data to parameterize the effect of spectral differences on echo detection in masking conditions, we did not include it in our model, thus simulating a conservative worst case scenario where all sounds lie

in the same frequency band. Additionally, attentional processes strongly improve target detection by improving the signal-to-noise ratio in the presence of maskers with similar time-frequency structure (57). Under real-world conditions, it is likely that masking in groups is even less than simulated here.

Due to the scarcity of published data, the interindividual and interspecific variation in the temporal and spatial masking functions used in our model is unknown. The temporal masking envelope will arguably be similar in many bat species, showing the typical mammalian pattern of worse target detection threshold with shorter temporal separation between target and masker. Spatial unmasking occurs through the nonlinear interaction of pinnae shape, cochlear and higher auditory processing (30, 58). As pinna shape and associated acoustic receiver characteristics strongly vary in echolocating bats (59), this will lead to species-specific spatial unmasking and echo detection rates in the sonar cocktail party nightmare.

Conclusion

We provide a conceptual framework to explain how active sensing animals such as echolocating bats successfully navigate in groups despite mutually jamming each other. The intense jamming in

groups might lead to individuals only detecting their nearest frontal neighbors, which might drive limited interactions within a group. We also show that call parameters and group geometry determine the challenge in the sonar cocktail party nightmare. Recent advances in on-body acoustic tags (42, 60), signal analysis (61), and acoustic tracking (62) of echolocating animals in the field might facilitate future experimental validation of our model predictions. As our model formulation is not constrained to echolocation in bats, it can be parametrized to other echolocators such as oilbirds, swiftlets, and odontocetes (63, 64) that also echolocate in groups and suffer from cocktail-party-like conditions.

ACKNOWLEDGMENTS. We thank the members of the Acoustic and Functional Ecology Group for insightful comments and support, Claire Guérin for contributing to code development, the Max Planck Institute for Ornithology for excellent research infrastructure, and 2 anonymous reviewers for helpful comments. T.B. was funded by a doctoral fellowship from the German Academic Exchange Service (DAAD) and the International Max Planck Research School for Organismal Biology. H.R.G. was funded by the Emmy Noether program of the German Research Foundation (DFG, GO 2091/2-1, GO 2091/2-2). The simulation runs in this paper were funded by a Google (Research Credits) grant to T.B.

1. M. E. Nelson, M. A. MacIver, Sensory acquisition in active sensing systems. *J. Comp. Physiol. A Neuroethol. Sens. Neural Behav. Physiol.* **192**, 573–586 (2006).
2. M. B. Fenton, Questions, ideas and tools: Lessons from bat echolocation. *Anim. Behav.* **85**, 869–879 (2013).
3. D. R. Griffin, *Listening in the Dark: The Acoustic Orientation of Bats and Men* (Yale University Press, New Haven, CT, 1958).
4. J. Matsubara, W. Heiligenberg, How well do electric fish electrolocate under jamming? *J. Comp. Physiol.* **125**, 285–290 (1978).
5. J. Ortega, Ed., *Sociality in Bats* (Springer International Publishing Switzerland, 2016).
6. T. H. Kunz, Ed., *Ecology of Bats* (Plenum Press, 1982).
7. E. C. Cherry, Some experiments on the recognition of speech, with one and with two ears. *J. Acoust. Soc. Am.* **25**, 975–979 (1953).
8. M. A. Bee, C. Micheyl, The cocktail party problem: What is it? How can it be solved? And why should animal behaviorists study it? *J. Comp. Psychol.* **122**, 235–251 (2008).
9. N. Ulanovsky, C. F. Moss, What the bat's voice tells the bat's brain. *Proc. Natl. Acad. Sci. U.S.A.* **105**, 8491–8498 (2008).
10. H. Brumm, H. Slabbekoorn, Acoustic communication in noise. *Adv. Stud. Behav.* **35**, 151–209 (2005).
11. E. Amichai, G. Blumrosen, Y. Yovel Calling louder and longer: How bats use biosonar under severe acoustic interference from other bats. *Proc. R. Soc. B Biol. Sci.* **282**, 20152064 (2015).
12. N. Cvikel et al., Bats aggregate to improve prey search but might be impaired when their density becomes too high. *Curr. Biol.* **25**, 206–211 (2015).
13. E. H. Gillam et al., Echolocation behavior of Brazilian free-tailed bats during dense emergence flights. *J. Mammal.* **91**, 967–975 (2010).
14. E. H. Gillam, B. K. Montero, Influence of call structure on the jamming avoidance response of echolocating bats. *J. Mammal.* **97**, 14–22 (2016).
15. Y. Lin, N. Abaid, R. Müller, Bats adjust their pulse emission rates with swarm size in the field. *J. Acoust. Soc. Am.* **140**, 4318–4325 (2016).
16. N. Ulanovsky, M. B. Fenton, A. Tsoar, C. Korine, Dynamics of jamming avoidance in echolocating bats. *Proc. Biol. Sci.* **271**, 1467–1475 (2004).
17. J. Habersetzer, Adaptive echolocation sounds in the bat *Rhinopoma hardwickei*. *J. Comp. Physiol.* **144**, 559–566 (1981).
18. G. Jones, M. Morton, P. M. Hughes, R. M. Budden, Echolocation, flight morphology and foraging strategies of some West African hipposiderid bats. *J. Zool.* **230**, 385–400 (1993).
19. J. Jarvis, W. Jackson, M. Smotherman, Groups of bats improve sonar efficiency through mutual suppression of pulse emissions. *Front. Physiol.* **4**, 140 (2013).
20. A. M. Adams, K. Davis, M. Smotherman, Suppression of emission rates improves sonar performance by flying bats. *Sci. Rep.* **7**, 41641 (2017).
21. B. Falk, L. Jakobsen, A. Surlykke, C. F. Moss, Bats coordinate sonar and flight behavior as they forage in open and cluttered environments. *J. Exp. Biol.* **217**, 4356–4364 (2014).
22. A. Surlykke et al., Echolocation in two very small bats from Thailand *Craseonycteris thonglongyai* and *Myotis siligorensis*. *Behav. Ecol. Sociobiol.* **33**, 1–12 (1993).
23. J. Tressler, M. S. Smotherman, Context-dependent effects of noise on echolocation pulse characteristics in free-tailed bats. *J. Comp. Physiol. A Neuroethol. Sens. Neural Behav. Physiol.* **195**, 923–934 (2009).
24. B. Möhl, A. Surlykke, Detection of sonar signals in the presence of pulses of masking noise by the echolocating bat, *Eptesicus fuscus*. *J. Comp. Physiol. A* **165**, 119–124 (1989).
25. Y. Lin, N. Abaid, Modeling perspectives on echolocation strategies inspired by bats flying in groups. *J. Theor. Biol.* **387**, 46–53 (2015).
26. M. L. Perkins, H. K. Frank, J. M. Pauly, E. A. Hadly, Frequency shifting reduces but does not eliminate acoustic interference between echolocating bats: A theoretical analysis. *J. Acoust. Soc. Am.* **142**, 2133–2142 (2017).
27. G. Jones, Scaling of echolocation call parameters in bats. *J. Exp. Biol.* **202**, 3359–3367 (1999).
28. D. R. Griffin, R. Galambos, The sensory basis of obstacle avoidance by flying bats. *J. Exp. Zool.* **86**, 481–506 (1941).
29. K. Hase et al., Bats enhance their call identities to solve the cocktail party problem. *Commun. Biol.* **1**, 39 (2018).
30. M. Ebata, Spatial unmasking and attention related to the cocktail party problem. *Acoust. Sci. Technol.* **24**, 208–219 (2003).
31. S. Sümer, A. Denzinger, H.-U. Schnitzler, Spatial unmasking in the echolocating big brown bat, *Eptesicus fuscus*. *J. Comp. Physiol. A Neuroethol. Sens. Neural Behav. Physiol.* **195**, 463–472 (2009).
32. W. A. Yost, *Fundamentals of Hearing: An Introduction* (Academic Press, London, 2007).
33. I. Siewert, T. Schillinger, S. Schmidt, “Forward masking and the consequence on echo perception in the gleaning bat, *Megaderma lyra*” in *Echolocation in Bats and Dolphins*, J. A. Thomas, C. F. Moss, M. Vater, Eds. (University of Chicago Press, 2004), pp. 266–268.
34. I. D. Couzin, J. Krause, R. James, G. D. Ruxton, N. R. Franks, Collective memory and spatial sorting in animal groups. *J. Theor. Biol.* **218**, 1–11 (2002).
35. G. Grégoire, H. Chaté, Onset of collective and cohesive motion. *Phys. Rev. Lett.* **92**, 025702 (2004).
36. T. Vicsek, A. Czirók, E. Ben-Jacob, I. Cohen, O. Shochet, Novel type of phase transition in a system of self-driven particles. *Phys. Rev. Lett.* **75**, 1226–1229 (1995).
37. C. W. Reynolds, Flocks, herds and schools: A distributed behavioral model. *ACM SIGGRAPH Comput. Graph.* **21**, 25–34 (1987).
38. D. J. T. Sumpter, The principles of collective animal behaviour. *Philos. Trans. R. Soc. Lond. B Biol. Sci.* **361**, 5–22 (2006).
39. T. Vicsek, A. Zafeiris, Collective motion. *Phys. Rep.* **517**, 71–140 (2012).
40. N. W. F. F. Bode, D. W. Franks, A. J. Wood, Limited interactions in flocks: Relating model simulations to empirical data. *J. R. Soc. Interface* **8**, 301–304 (2011).
41. M. Ballerini et al., Interaction ruling animal collective behavior depends on topological rather than metric distance: Evidence from a field study. *Proc. Natl. Acad. Sci. U.S.A.* **105**, 1232–1237 (2008).
42. N. Cvikel et al., On-board recordings reveal no jamming avoidance in wild bats. *Proc. R. Soc. B Biol. Sci.* **282**, 20142274 (2015).
43. J. Luo, H. R. Goerlitz, H. Brumm, L. Wiegrebe, Linking the sender to the receiver: Vocal adjustments by bats to maintain signal detection in noise. *Sci. Rep.* **5**, 18556 (2015).
44. K. Hase, T. Miyamoto, K. I. Kobayashi, S. Hiryu, Rapid frequency control of sonar sounds by the FM bat, *Miniopterus fuliginosus*, in response to spectral overlap. *Behav. Processes* **128**, 126–133 (2016).
45. G. A. Miller, J. C. R. Licklider, The intelligibility of interrupted speech. *J. Acoust.* **22**, 167–173 (1950).
46. A. Surlykke, Target ranging and the role of time-frequency structure of synthetic echoes in big brown bats, *Eptesicus fuscus*. *J. Comp. Physiol. A* **170**, 83–92 (1992).
47. A. E. Petrides, O. S. Eng, D. S. Mowles, J. A. Simmons, C. M. DeLong, Interpulse interval modulation by echolocating big brown bats (*Eptesicus fuscus*) in different densities of obstacle clutter. *J. Comp. Physiol. A Neuroethol. Sens. Neural Behav. Physiol.* **195**, 603–617 (2009).
48. M. E. Bates, S. A. Stamper, J. A. Simmons, Jamming avoidance response of big brown bats in target detection. *J. Exp. Biol.* **211**, 106–113 (2008).
49. J. Luo, C. F. Moss, Echolocating bats rely on audiovocal feedback to adapt sonar signal design. *Proc. Natl. Acad. Sci. U.S.A.* **114**, 10978–10983 (2017).
50. A. J. Corcoran, C. F. Moss, Sensing in a noisy world: Lessons from auditory specialists, echolocating bats. *J. Exp. Biol.* **220**, 4554–4566 (2017).
51. J. A. Simmons, J. E. Gaudette, Biosonar echo processing by frequency-modulated bats. *IEE Radar Sonar & Navigation* **6**, 556–565 (2012).
52. K. Ghose, T. K. Horiuchi, P. S. Krishnaprasad, C. F. Moss, Echolocating bats use a nearly time-optimal strategy to intercept prey. *PLoS Biol.* **4**, e108 (2006).

53. K. Ghose, C. F. Moss, Steering by hearing: a bat's acoustic gaze is linked to its flight motor output by a delayed, adaptive linear law. *J. Neurosci.* **26**, 1704–1710 (2006).
54. Y. Yovel, M. L. Melcon, M. O. Franz, A. Denzinger, H. U. Schnitzler, The voice of bats: How greater mouse-eared bats recognize individuals based on their echolocation calls. *PLOS Comput. Biol.* **5**, e1000400 (2009).
55. H. Fletcher, Auditory patterns. *Rev. Mod. Phys.* **12**, 47–66 (1940).
56. R. R. Fay, "Sound source perception and stream segregation in nonhuman vertebrate animals" in *Auditory Perception of Sound Sources*, W. A. Yost, A. N. Popper, R. R. Fay, Eds. (Springer Science+Business Media, LLC, 2008), pp. 307–323.
57. E. R. Hafter, A. Sarampalis, P. Loui, "Auditory attention and filters" in *Auditory Perception of Sound Sources*, W. A. Yost, A. N. Popper, R. R. Fay, Eds. (Springer Science+Business Media, LLC, 2008), pp. 115–142.
58. J. F. Culling, M. A. Stone, "Energetic masking and masking release" in *The Auditory System and the Cocktail Party*, J. C. Middlebrooks, J. Z. Simon, A. N. Popper, R. R. Fay, Eds. (ASA Press, 2017), pp. 41–74.
59. M. K. Obrist, M. B. Fenton, J. L. Eger, P. A. Schlegel, What ears do for bats: a comparative study of pinna sound pressure transformation in chiroptera. *J. Exp. Biol.* **180**, 119–152 (1993).
60. L. Stidsholt *et al.*, A 2.6-g sound and movement tag for studying the acoustic scene and kinematics of echolocating bats. *Methods Ecol. Evol.* **10**, 48–58 (2018).
61. O. Mac Aodha *et al.*, Bat detective-deep learning tools for bat acoustic signal detection. *PLOS Comput. Biol.* **14**, e1005995 (2018).
62. A. M. Seibert, J. C. Koblitz, A. Denzinger, H. U. Schnitzler, Bidirectional echolocation in the bat *Barbastella barbastellus*: Different signals of low source level are emitted upward through the nose and downward through the mouth. *PLoS One* **10**, e0135590 (2015).
63. S. Brinklov, M. B. Fenton, J. M. Ratcliffe, Echolocation in oilbirds and swiftlets. *Front. Physiol.* **4**, 123 (2013).
64. A. Surlykke, P. E. Nachtigall, R. R. Fay, A. N. Popper, Eds., *Biosonar* (Springer-Verlag, New York, 2014).



Supplementary Information for

Modeling active sensing reveals echo detection even in large groups of bats

Thejasvi Beleyur, Holger R. Goerlitz

Email: thejasvib@gmail.com, hgoerlitz@orn.mpg.de

This PDF file includes:

- Supplementary methods
- Schematic S1
- Tables S1 to S2
- Figures S1 to S5
- SI References

SUPPLEMENTARY METHODS

1. Model parametrization

Here, we present the details of how we parametrized our model of the sonar cocktail party nightmare, based on empirical data of behavioral studies in bats and our own measurements.

1.1 Temporal masking envelope

We derived the echo-to-masker sound pressure level (SPL) ratios for forward, backward and simultaneous masking from two empirical target-detection studies in echolocating bats (**Table S1**). We only chose studies where the target and masker were co-located along the same direction. Both studies presented the ratio between the echo and masker SPL at target detection for various delays between echo and masker arrival time. We linearly interpolated (in a piecewise fashion) the echo-to-masker SPL ratios between each of the time delays measured in the studies to obtain the full temporal masking envelope ranging from -0.65 and +24 ms delay of the target echo relative to the masker edge (**Fig. S1**).

1.2 Spatial unmasking function

Sümer et al., 2009 (1) performed a backward masking study to address spatial unmasking in the bat *Eptesicus fuscus*. In a two-alternative forced-choice paradigm, they increased the angular separation between a target object and a masker object while also varying the level of the target object's echo (by varying the size of the target object and thus the target object's target strength).

We define the spatial unmasking function as the echo-to-masker SPL ratio at just-noticeable echo detection as a function of angular separation. To obtain the echo-to-masker level ratios, we subtracted the target object's target strengths from the masker object's target strength. We normalized the spatial unmasking function to the co-localised echo-masker case (i.e., when both echo and masker arrive from the same direction). This describes the reduction in echo-to-masker ratio required for echo detection as a function of angular separation between target and masker,

compared to the co-localized case. We digitized the data points from Fig. 4B of Sümer et al. (2009) by hand with WebPlotDigitiser (2) to obtain the target's target strength as a function of angular separation. Masker target strength was given by Sümer et al. (2009) as -14.5 dB. We then calculated the target-masker SPL ratios and interpolated them with a quadratic polynomial fit (**Fig S2**). The interpolated data was then further upsampled to 0.47° intervals. As Sümer et al. (2009) only measured angular separations up to 23°. We conservatively used the echo-masker SPL ratio at 23° also for all larger angular separations.

1.3 Call and hearing directionality

Echolocation calls have a directional beam shape, meaning that the emitted SPL generally decreases with increasing angular distance from the main call direction, which has the highest call SPL (**Fig. S3**). The highest call SPL is typically towards the front, and reduces towards the back of the bat. Despite this directionality and additional variation with call frequency and behavioral context (3–6), bats still emit a significant amount of sound pressure into the backward direction. The average call SPL behind a bat is about 14 dB lower than in the forward direction (6, 7). Call directionality leads to a drop in the effective number of masking calls from neighbors as only those calls arriving from a limited range of directions will have sufficiently high SPL (**Fig. S3**). For example, in an emergence situation with approximately parallel flight directions, the focal bat will receive the loudest calls from those bats flying behind it. Similarly, the lowest received call levels in an emergence will be from those bats flying in front of the focal bats.

Like call production, hearing is also directional. The pinna structure of a bat attenuates or amplifies the same sound depending on its direction of arrival (8, 9). In *Myotis daubentonii*, hearing directionality between 35-45 kHz leads to an average amplification of frontally arriving sounds by 4 dB in comparison to those arriving from behind. We used data of Giuggioli et al (2015) to describe the average call and hearing directionality of our modelled bats (**Fig. S3**).

1.4 Atmospheric attenuation

Ultrasound in air is heavily attenuated by atmospheric attenuation, even over short distances of a few meters (10, 11). Atmospheric attenuation will reduce the received SPL of a masker or echo at the focal bat. We chose a range of values for the atmospheric attenuation coefficient α between 0 to -2 dB/m. These values approximate the atmospheric attenuation experienced by a bat calling at very low (≤ 20 kHz, ~ 0 dB/m) to high (60 kHz, ~ -2 dB/m) peak frequencies.

1.5 Geometric attenuation

Sound pressure level reduces with increasing distance from the source, called geometric attenuation. For all sounds in our model (target echoes, masking calls and secondary echoes), we implemented spherical geometric spreading, i.e., uniform spreading of sound in all directions (12).

1.6 Group geometry

A group of bats might organize themselves tightly or well spread in the field. The spacing between bats will decide how loud the returning target echoes, masking calls and secondary echoes are. We simulated a group of bats by placing individual bats on a 2D plane using the Poisson disk algorithm (13). The advantage of using the Poisson disk algorithm is that points are spaced relatively uniformly in space compared to a random placement of points from two independent distributions. The other advantage of the Poisson disk algorithm is that it allows the specification of a minimum distance between two points. For the first simulations varying group size only, we chose 0.5 m as inter-bat distance (see Table 1, main text), matching the average interbat-distance in dense swarms of *T. brasiliensis* in the field (14). In addition to 0.5 m minimum inter-bat distance, we also studied how a sparser 1.0 m minimum inter-bat distance affects neighbor detection (see Table 1, main text). The Poisson disk arranged bats showed average inter-bat distances of between 1-1.5 times the specified minimum distance between points.

1.7 Heading variation

Active sensing animals are known to 'scan' their environments by emitting energy in varying directions of interest according to the behavioral context (15, 16). Bats alter the shape and direction of their sonar beam while they fly (3, 17, 18). The directions into which each bat in a group aims its calls could affect how well each bat in the group can detect echoes. A group of bats calling into the same direction may experience high masking, as a focal individual will receive many loud calls from the bats behind it. In contrast, a group of bats calling into a larger range of directions may experience less masking. The focal bat may receive a mix of fainter off-axis calls and loud on-axis calls from neighbors.

We simulated the scanning behavior of individual bats in the group by setting a heading angle for each individual. Each individual called into the direction of its heading angle, and we chose two levels of variation of heading angles in the group. Groups with a low heading variation were all pointing their beams in more or less the same direction. Groups with high heading variation were pointing their beams in a wider range of directions. A low heading variation simulates an emergence situation where each bat is calling approximately into the overall flight direction of the group. A high heading variation simulates a swarming situation where each bat is calling at a unique direction. Given the lack of empirical data to guide our estimates, we chose $\pm 10^\circ$ for the low heading variation, and $\pm 90^\circ$ for the high heading variation. The heading angle for each individual was randomly drawn from a uniform distribution covering the respective range.

1.8 Monostatic and bistatic target strength of a flying bat

Quantifying the received levels of echoes and secondary echoes requires knowledge of the target strength of a bat when emitter and receiver are at the same and at different locations. Here, we measured monostatic and bistatic target strengths (19) of a flying stuffed *Myotis myotis* bat. Monostatic target strengths refer to the situation where the emitter and receiver are at the same location, i.e., they are the same bat (this is the 'classical' target strength usually considered in echolocation research). Bistatic target strength refers to a situation where the

emitter and receiver are at different locations, i.e., the receiving bat hears the echo of a call that was emitted by another bat, i.e. a secondary echo.

In the simulations, all incoming and outgoing sounds at the bat are between $\text{abs}(0-180)^\circ$. Sounds with 0° angle are along the heading direction of the focal bat. Sounds arriving/reflecting on the left have negative angles ($0 \geq \theta \geq -180^\circ$), and those on the right have positive angles ($0 \leq \theta \leq 180^\circ$).

Methods: We ensonified a stuffed *Myotis myotis* with outstretched wings, which was suspended from the ceiling at ~1 m height and placed on a rotating base, which could be rotated in 45° steps. A speaker (electrostatic Polaroid, custom built) and microphone (CM16/CMPA, Avisoft Bioacoustics, Glienicke, Germany) were placed at a 1 m radial distance to the center of the bat (**Fig. S4**). The speaker emitted linear frequency modulated sweeps between 96-20 kHz, with durations of 170 μs , 1 ms and 2 ms at 92 dB rms SPL re 20 μPa at 1 m. The speaker was driven by a custom-built amplifier with input from a soundcard (Player 216H, Avisoft Bioacoustics, 1 MHz sampling rate). The microphone signal was recorded simultaneously with an attenuated version of the speaker signal on a multichannel soundcard (USG 416H, Avisoft Bioacoustics, 500 kHz sampling rate). The microphone had a noise floor of 24 dB rms SPL re 20 μPa . All echoes were recorded at $\geq 22\text{dB}$ signal-to-noise ratio. The experiment was performed in the middle of a large empty room (~4x4x2 m) to temporally separate bat echoes from background echoes.

We ensonified the bat from front (0°) to back (180°) in steps of 45° . We assumed that the bat was symmetrical and thus did not ensonify angles from $180-360^\circ$. The angular separation between the speaker and the microphone was also altered in steps of 45° between -180° to $+180^\circ$. This resulted in 40 target strength measurements (5 sound directions x 8 angular separations).

The integrated target strength (20) of the recordings were calculated by subtracting the energy of recordings with the bat from those without the bat at the expected time window of echo arrival. The echo level was calculated in rms by taking the square root of the energy.

Results: The monostatic target strength of a flying stuffed *Myotis myotis* bat at various orientations was between -43 and -34 dB at 1 m distance, matching the general range of previously published values (21). The bistatic target strength, which was used to calculate the received level of the secondary echoes, was between -44 and -10 dB across all combinations of emitter-receiver locations.

For further details on experimental protocol, raw data and reproduction of generated results, please refer to the archived Jupyter notebooks at this link: <https://doi.org/10.5281/zenodo.3469845>.

1.9 Acoustic shadowing in bat groups with varying number of bats and inter-bat spacing

As multiple bats fly together in a group, the bats themselves will block all sounds travelling between an emitter and a receiver. Essentially, the bats themselves act as obstacles that cause acoustic shadowing, reducing the received sound pressure level at the focal bat. In a large group, multiple bats may shadow a sound as it moves from the emitter and to the receiver. We quantified acoustic shadowing in a series of playback experiments that varied the inter-bat spacing (0.5 and 1.0 m) and the number of bats (1 – 6) in a line.

Methods: A microphone (CM16/COMPA, Avisoft Bioacoustics) and speaker (Polaroid, custom-built) were placed at a fixed distance of 9.9 m apart, facing each other. We hung 1 to 6 “model bats” made of foam with paper wings at 0.5 or 1.0 m distance to each other from a string running above the speaker to the microphone. The designed model bat showed acoustic shadowing similar to that of the stuffed *Myotis myotis* used in the target strength measurements described in 1.8.

The speaker was placed as far as possible from the microphone to calculate acoustic shadowing without the effects of speaker directionality. The speaker played back a variety of 7 ms Tukey windowed signals consisting of pure tones (20, 35, 50, 100 kHz) and a downward modulated linear sweep (100-15 kHz). Each signal type was played back 15 times at ~4% duty cycle. Multiple signal types were used to obtain a generalized estimate of shadowing across a wide range of call

peak frequencies and call types. The playback signals and recordings are available here: <https://doi.org/10.5281/zenodo.3469845>. Additionally, we also recorded the same playback without model bats being present. We calculated acoustic shadowing as the reduction in received level by subtracting the received level (in dB rms) without bats from the received level with bats. We performed a linear regression of attenuation as a function of factors *number of bats* and *inter-bat-distance*, to estimate the amount of acoustic shadowing caused per bat and the spacing between them.

Results: Bats effectively shadowed the sound, with strong effects of the inter-bat-spacing and the number of bats. Bats at 0.5 m distance in front of the receiving bat (=microphone) reduced the received SPL by 5.17 dB (SEM=0.44, $t=-11.639$, 95% CI =-6.05,-4.30), while bats at 1.0 m interbat-spacing reduced the received SPL by 1.85 dB (SEM=0.44, $t=-4.164$, 95% CI =-2.72,-0.98). Each bat reduced received SPL by 0.83 dB (SEM=0.08, $t=-9.852$, 95% CI =-0.99,-0.66).

For further details on experimental protocol, raw data and reproduction of generated results, please refer to the archived Jupyter notebooks at this link: <https://doi.org/10.5281/zenodo.3469845>.

2. Model implementation

Here, we present how we implemented the parameters described before into our final model, and how our model was initialized and run.

2.1 Model idea

The idea of our model is to analyze the relative timing and sound pressure level of target echoes, masking calls and secondary echoes at a focal bat flying in a group of other bats. Each model iteration thus analyzed one single interpulse interval, i.e., the time after emission of one call until the emission of the next call by the focal bat. Within that interpulse interval, the focal bat received the echoes from its own call that reflected off the neighboring bats, the calls of those

neighboring bats, and the secondary echoes which originate from the calls of the neighboring bats reflecting off other neighboring bats (Figure 1, main text).

We placed groups of bats in a 2D plane with various inter-bat distances and heading directions. We then calculated received timing and SPL of all sounds based on realistic assumptions about call properties, mammalian auditory characteristics and sound physics.

All echoes, calls and secondary echoes were considered to be equal in duration, amplitude envelope, and frequency composition. Frequency composition was not explicitly specified, which is a conservative modelling choice that maximizes masking potential (22) and makes our model generalizable to multiple bat species. All sounds were treated as having a constant amplitude envelope (i.e., no amplitude modulations), but they differed in the sound pressure level received by the focal bat.

2.2 Model initialization

Each model iteration consisted of distributing bats in a 2D plane and assigning each bat a heading direction. This spatial distribution was used to calculate the arrival times and received level of target echoes, masker calls and secondary echoes within the interpulse interval (**Fig. 1**). The interpulse interval was discretized into time bins of 1 μ s duration. Each received target echo corresponded to one neighbor. The arrival time of each echo was calculated using twice the distance between focal and neighboring bat.

The arrival time of masker calls and secondary echoes were chosen randomly. The random arrival time assignment of masker calls and secondary echoes is supported by the finding that groups of *Miniopterus fuliginosus* (23) do not coordinate their calling behavior, and seem to echolocate independently. Moreover, at large group sizes beyond a few bats it is unlikely that bats could effectively co-ordinate their call emission times.

2.3 Target echo properties

Target echoes are the echoes that the focal bat receives in response to its own echolocation call. In our model, the target echoes are echoes reflected off the neighboring bats. When a focal bat hears a target echo it means it has detected the corresponding neighboring bat.

An echo was defined as a sound occupying a block of time within the interpulse interval (**Fig. S5A**). Echoes were simulated to arrive at delays corresponding to the distance to the neighboring bat they reflected off, e.g. if a neighboring bat was at 1 m distance to the focal bat, then its echo arrived at a delay of 6.06 ms (at 330 m/s sound propagation).

The received level of the returning echo was calculated based on emitted call source level into the direction of the neighboring bat, our monostatic target strength measurements of a bat, and geometric attenuation over the sound travel distance. If acoustic shadowing and atmospheric absorption were included in a simulation run, the received level was reduced based on the number of bats in the path and the atmospheric attenuation for the overall distance travelled by the echo. Echo arrival direction was determined based on the position of each neighboring bat.

2.4 Masker call properties

Masker calls arrived at random time points with uniform probability within the interpulse interval (**Fig. S5,B**), based on the observed lack of call synchronization in groups of *Miniopterus fuliginosus* (23). Call directionality was based on the directionality function in Giuggioli et al., 2015, who fit a cosine based function to describe the overall call directionality of *Myotis daubentonii* echolocating in the field. We set the asymmetry parameter A to 7.0. We calculated the angle of call emission towards the focal bat for each conspecific bat based on its angular position (heading) and distance. We then calculated the effective source level into the direction of the focal bat by reducing the call's on-axis source level (**Table 1 in main text**) according to the call directionality function and the focal bat's relative position to the conspecific (**Fig. S3**). This reduced level was the final received level of the conspecific masker call. If acoustic shadowing and atmospheric attenuation

were included in a simulation run, the received level was reduced based on the number of bats in the path and the overall distance travelled by the call.

2.5 Secondary echo properties

Like the masking calls, secondary echoes arrived randomly with uniform probability in the interpulse interval (**Fig. S5C**). The received level of a secondary echo was based on the emitted call source level into the direction of the neighboring bat, our bistatic target strength measurements of a bat, and geometric attenuation over the sound travel distance. If acoustic shadowing and atmospheric absorption were included in a simulation run, the received level was reduced based on the number of bats in the path and the overall distance travelled by the secondary echo.

2.6 Obtaining the masker sound pressure level profile

All sounds were treated as having a fixed received level (no envelope modulations). For each target echo, we calculated its unique masker SPL profile based on the relative timing, relative arrival directions and received levels of all masking calls and secondary echoes. This masker SPL profile was different for each target echo because the temporal and spatial properties of the masking sounds differ for each echo, resulting in different received levels and spatial unmasking (see main text for details). We first calculated the effective masker SPL for each masking sound by correcting for spatial unmasking based on the angular separation between the echo and the masker. All effective masker SPLs of all masking sounds together over time represent the complete masker sound pressure profile for each target echo (**Fig. S5,E**). When two or more maskers overlapped in time, we added their linear sound pressures to obtain their joint masking SPL. This approach assumes that overlapping maskers are coherent sound sources that constructively interfere. This is a conservative assumption that will maximize masking.

2.7 Determining neighbor detection: the temporal masking envelope

The masker SPL profile for each echo describes the received masking SPL over time. From the masker SPL profile, we created an echo-to-masker ratio profile by normalizing the SPL of the target echo to the masker SPL profile:

$$\begin{aligned} & \text{echo-to-masker ratio profile (dB)} \\ &= \text{echo level (dB SPL)} - \text{masker sound pressure profile (dB SPL)} \end{aligned}$$

The echo-to-masker-ratio profile is comparable to a signal-to-noise-ratio: at 0 dB, echo and masker have the same SPL. The masker is louder than the echo for negative values, and the echo is louder than the masker for positive values.

To determine whether a given target echo was heard or not, we compared the echo-to-masker ratio for this echo with the temporal masking envelope (see 1.1). The temporal masking envelope describes the echo-to-masker ratio at which masking occurs as a function of relative timing between echo and masker. Using the temporal masking envelope is important because masking does not only occur when the masker coincides with the echo, but also when the masker does not overlap with the echo and arrives before (forward masking) or after (backward masking) it. In our case, echo and masker had durations of only 1-2.5 ms, while a masker arriving at up to ~25 ms before and up to ~1 ms after the echo still causes some amount of masking. Thus, our temporal masker envelope had a duration of either ~27 or ~28.5 ms (**Fig. S5F**). We compared the echo-to-masker ratio profile to the temporal masking envelope. The echo was considered not heard if the echo-to-masker ratio profile lay below the temporal masking envelope, i.e., the echo-to-masker ratio was lower than required for echo detection. Alternatively, the echo was considered heard if the echo-to-masker ratio profile lay above the temporal masking function, i.e., the echo-to-masker SPL ratio was higher than required for echo detection.

However, as the echo-to-masker ratio continuously fluctuates over time, it is possible that it is not fully above or below the temporal masking envelope throughout the envelope's duration. We thus defined an echo to be masked (= not

heard), if it was masked for more than 25% of its duration (of 1 or 2.5 ms). To calculate the total duration of masking, we analyzed the total duration that the echo-to-masker ratio was below the temporal masking envelope.. As long as the total masking duration was shorter than 25% of the echo duration (of 1-2.5 ms) the echo was considered detected. If this duration was longer than 25% of the echo duration, the echo was masked and the corresponding neighboring bat was considered not detected. This 25% threshold was set to make the simulated auditory system immune to short spikes in masking sound pressure level occurring during the temporal masking function.

3. Open-source software used in the research

All simulation code, experimental data and results were made possible through the use of the NumPy (24), SciPy (25), Pandas (26), Matplotlib (27), Statsmodels (28), sounddevice (29), Anaconda (30) and CPython (31) open-source projects.

4. Acknowledgements

We thank Renate Heckel and Felix Hartl for contributing to and building the ensonification setup, Magnus Wahlberg for helpful discussions on the ensonifications, Henrik Brumm for permission to use Raum 1.03 for the ensonification experiments, and Mihai Valcu for facilitating simulation runs on the in-house server facility.

5. Supplementary Schematics, Tables and Figures

Schematic 1: Pseudo-code of the steps in a simulation run to determine the detected neighbors per call emission.

1. Place N bats in group with minimum inter-bat distance
2. Choose bat closest to the center of the group as the focal bat
3. Populate interpulse intervals with maskers and echoes:
 - a. Propagate maskers (calls and secondary echoes) and calculate their received levels according to the position and orientation of the source neighbors. Assign random timing within interpulse interval.
 - b. Propagate echoes from focal bats' own call and calculate their arrival time and received levels according to the position and orientation of the neighbors.
4. Implement hearing directionality of the focal bat: amplify the received level of all sounds according to their relative angle of arrival
5. Per echo, determine if it was heard:
 - a. Implement spatial unmasking by reducing the effective received level of all masking sounds based on their angular separation to the echo
 - b. Combine all maskers over time to form a 'masker profile'
 - c. Calculate the echo-to-masker profile', with reference to the echo level
 - d. Implement temporal masking by checking if the relative echo-masker profile lies below the temporal masking envelope centered on the echo's location in the interpulse interval.

Table S1: Target-detection studies in echolocating bats used to extract echo-masker SPL ratio for our model. The time delay is the time between the edge of a masker and the target echo. A positive time delay indicates forward masking (masker arrives before the target), a negative time delay indicates backward masking (masker arrives after the target).

Publication	Study species	Time delay (ms)	Masking condition	Echo-masker SPL ratio (dB)
Siewert et al. (2000) (32)	<i>Megaderma lyra</i>	3	Forward	-17
		6	Forward	-23
		12	Forward	-29
		24	Forward	-34
Sümer et al. (2009) (1)	<i>Eptesicus fuscus</i>	-0.65	Backward	-22.3

Table S2: Results of the logistic regression to quantify the effect of different parameter values on the odds ratio to detect at least one neighbor. Odds ratio values >1 indicate a higher probability of neighbor detection, while odds ratios <1 indicate a lower probability of neighbor detection.

Parameter	Value tested	Reference value	Odds Ratio	Odds ratio-2.5 CI	Odds ratio-97.5 CI	Log Odds ratio	Log Odds ratio SEM	Z (log odds ratio estimate)	P > z
Intercept			0.32	0.31	0.35	-1.11	0.027	-40.51	0.0
Heading variation (°)	±90	±10	1.32	1.28	1.36	0.28	0.015	18.35	0.0
Acoustic shadowing	Yes	no	0.75	0.73	0.78	-0.28	0.015	-18.63	0.0
Interpulse interval (ms)	25	100	0.001	0.0009	0.001	-6.84	0.073	-93.52	0.0
	50	100	0.048	0.046	0.050	-3.04	0.023	-134.14	0.0
	200	100	14.60	13.995	15.228	2.68	0.022	124.46	0.0
	300	100	74.68	70.497	79.122	4.31	0.029	146.49	0.0
Minimum interbat distance (m)	1.0	0.5	0.31	0.301	0.321	-1.17	0.016	-72.83	0.0
Sound duration (ms)	1	2.5	34.66	33.172	36.206	3.55	0.022	158.83	0.0
Source Level (dB SPL re 20 µPa at 1m)	94	100	0.99	0.941	1.034	-0.01	0.024	-0.57	0.57
	106	100	1.01	0.966	1.061	0.01	0.024	0.52	0.60
	112	100	1.01	0.966	1.061	0.01	0.024	0.50	0.62
	120	100	0.98	0.938	1.030	-0.02	0.024	0.73	0.47
Atmospheric attenuation (dB/m)	0	-1	1.05	1.010	1.086	0.05	0.019	2.48	0.01
	-2	-1	1.01	0.970	1.042	0.01	0.018	0.27	0.78

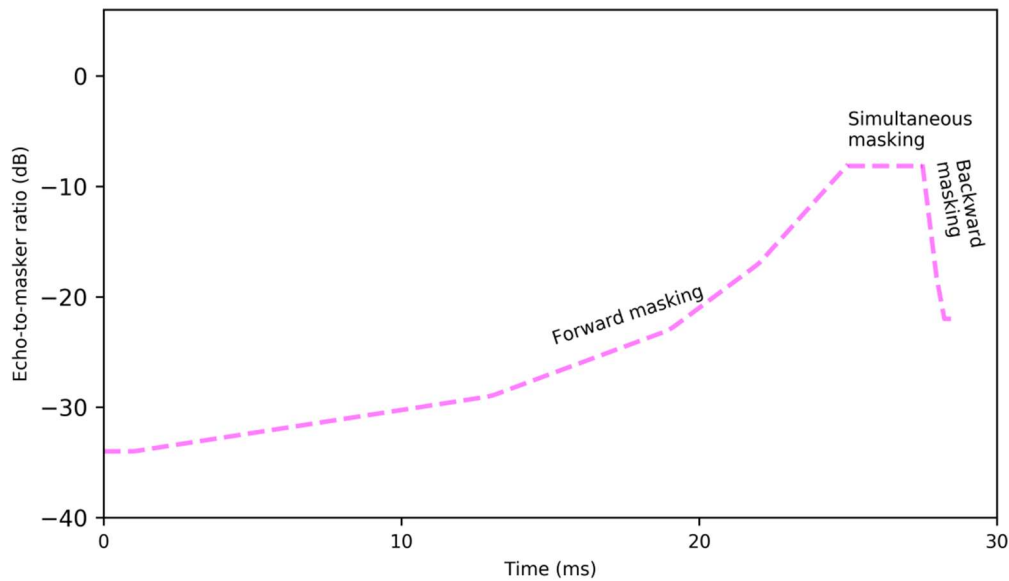


Figure S1: The 'temporal masking envelope' used to simulate temporal masking. The envelope represents the lower echo-to-masker ratios at which a bat can detect echoes for various echo-masker delays. The envelope is the equivalent of the lowest signal-to-noise ratios at which echoes can be detected over different time delays. The envelope is centered on the position of the echo, and has a long forward masking section (at times prior to the echo), and a short backward masking section (at times after the echo). The simultaneous masking region is equal to the length of the echo itself. If the echo-to-masker ratio profile is above the temporal masking envelope for most of its duration (i.e., the echo-to-masker SPL ratio was higher than required for echo detection), we considered an echo to be heard. If the echo-to-masker ratio profile is below the envelope for more than 25% of the echo's duration, the echo was considered not heard. Here the temporal masking envelope is shown for a 2.5 ms echo. Data and sources used to construct the temporal masking envelope are given in Table S1.

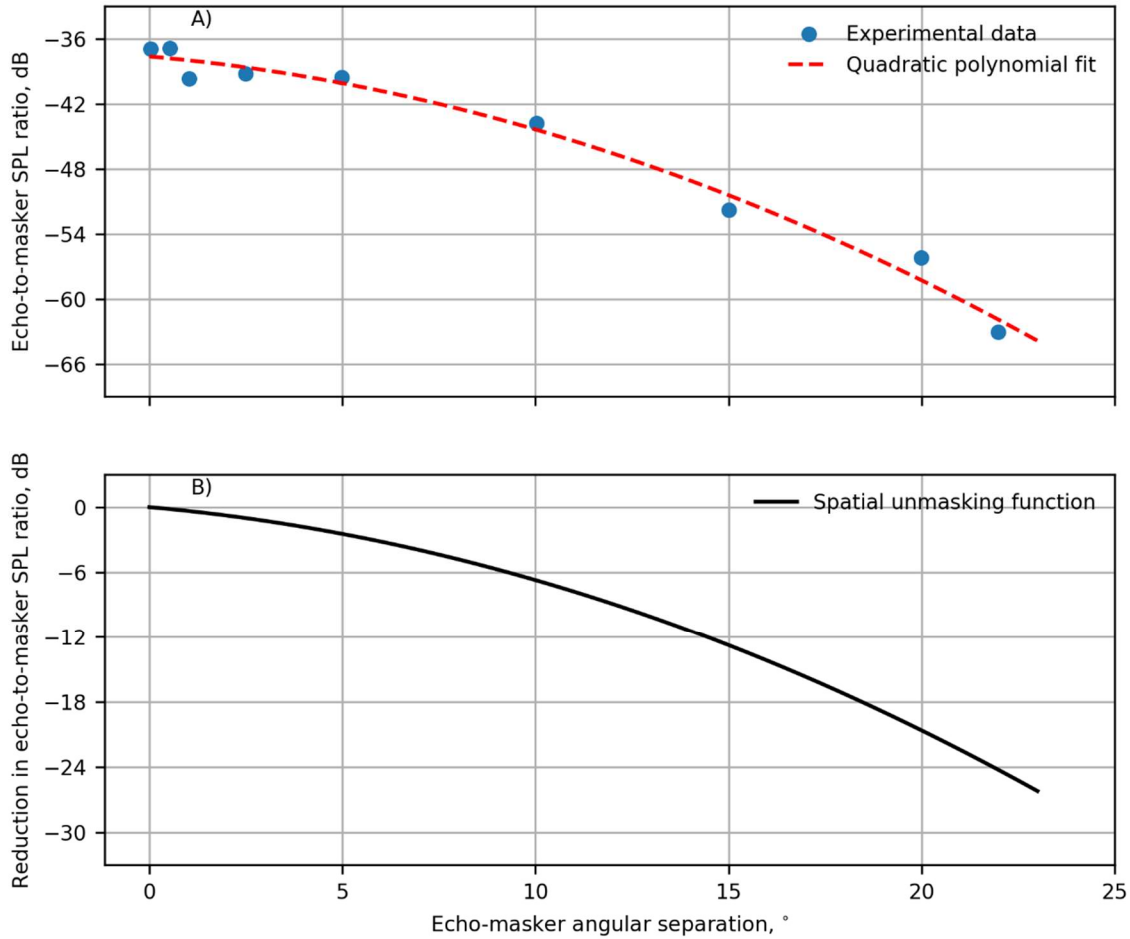


Figure S2: The ‘spatial unmasking function’ describes the reduction in echo-to-masker SPL ratio at echo detection as a function of angular separation between echo and masker.

A) The original data set of Sümer et al. (2009) (blue dot) and our digitized and interpolated dataset (red line). The error between the data and our interpolation is less than 2 dB.

B) The final spatial unmasking function as used in our simulations was derived from the interpolated fit in A), which was normalised to the echo-to-masker ratio at zero degrees angular separation. This final spatial unmasking function describes the reduction in required echo-to-masker SPL ratio relative to the co-localized case: when echo and masker are co-localized, the reduction is 0 dB, while the reduction becomes greater with increasing angular separation.

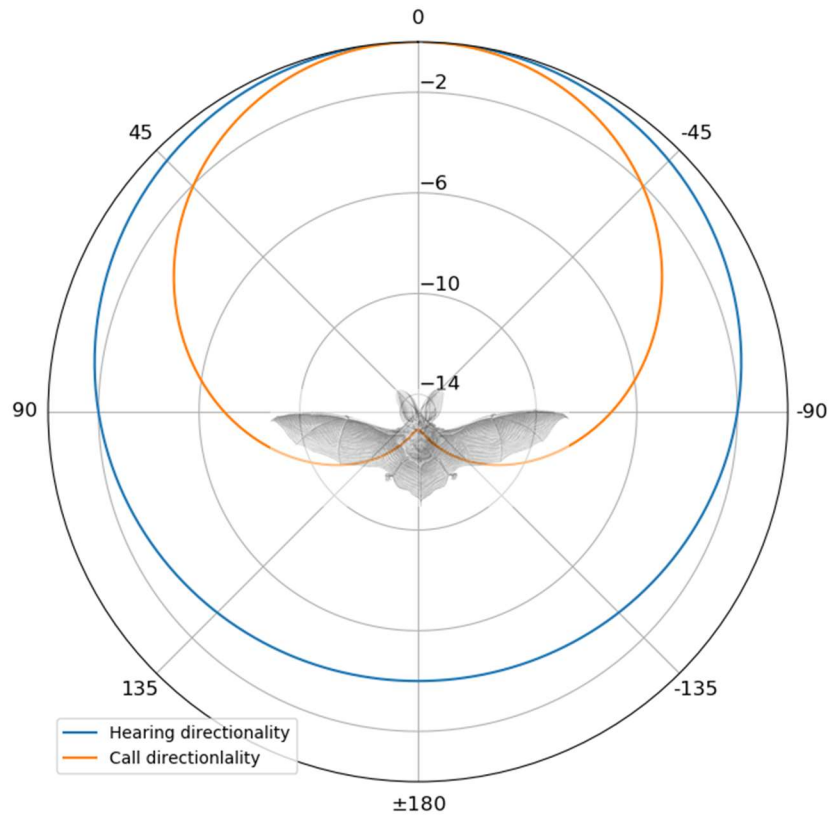


Figure S3: Calling and hearing directionality of bats. Call directionality (orange) is directional, with a difference of up to -14 dB in source level from front to back. Calls emitted to the front of a bat result in higher received levels of calls, echoes and secondary echoes. Hearing directionality (blue) is less directional, with a difference of up to -4 dB from front to back. Hearing directionality causes sounds arriving from the back to be perceived fainter than sounds arriving from the front. Bat drawing from *Kunstformen der Natur* (Ernst Haeckel, 1899).

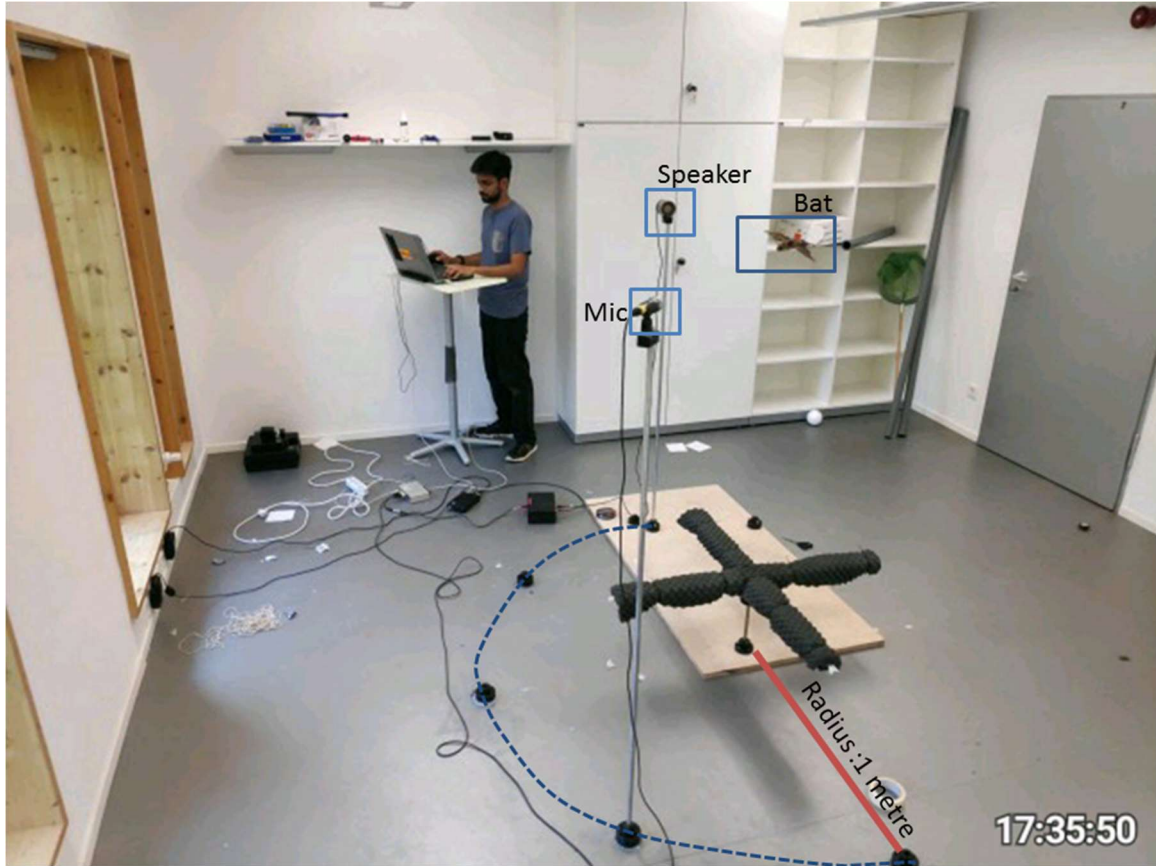


Figure S4: The ensonification setup used to measure the monostatic and bistatic target strength of a bat as an acoustic target. A stuffed *Myotis myotis* bat was hung at the same height as the speaker and microphone. The bat could be rotated in the azimuth. The microphone and speaker were placed at 1 m radius around the bat at various positions (black rounded plastic molds on floor) with a separation of 45° from each other. By a combination of bat orientation, microphone and speaker positions all possible incoming and outgoing relative angles were measured. Here the positions of the speaker and microphone for a bistatic target strength measurement with 135° angle between microphone and speaker are shown.

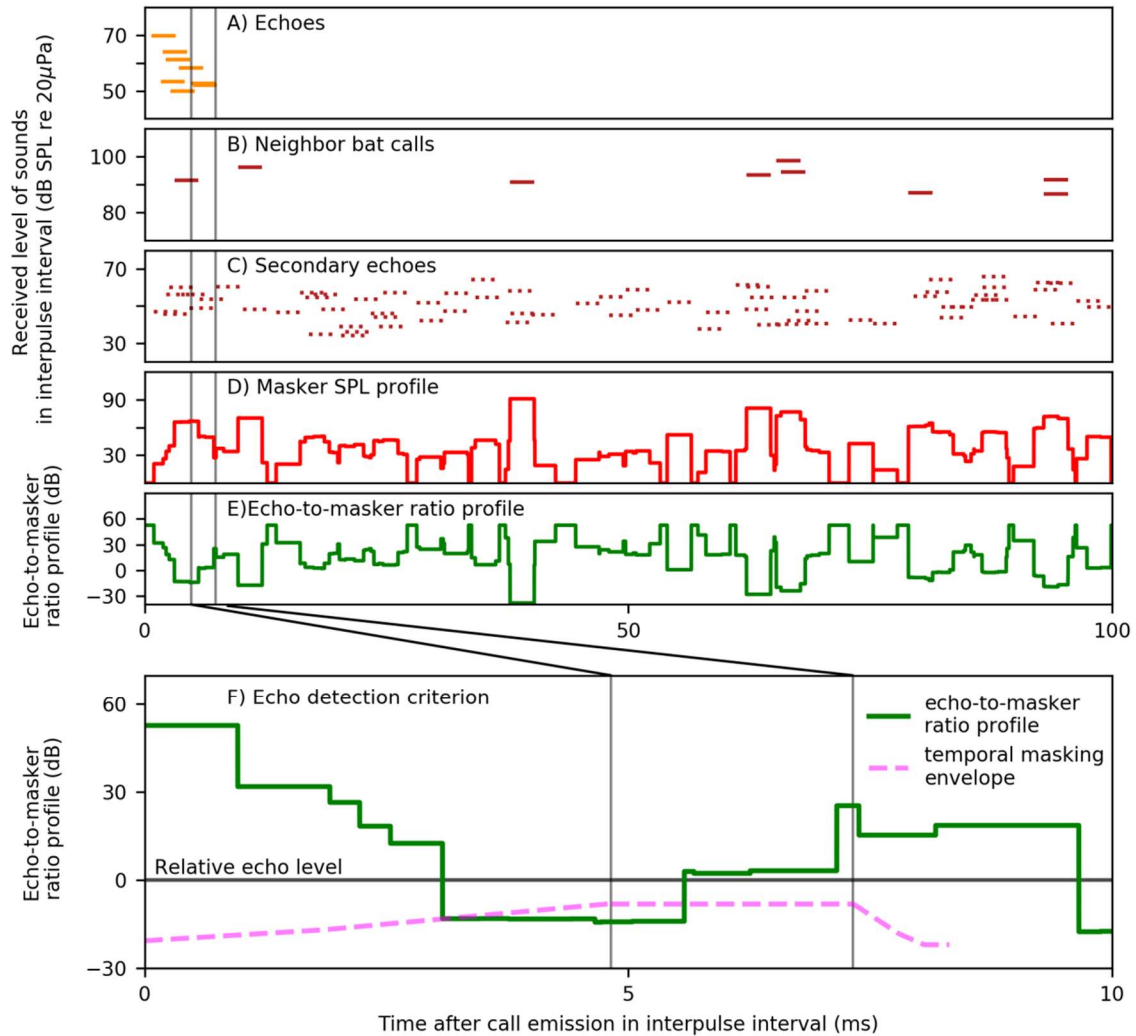


Figure S5: Schematic representation of the sounds arriving in the interpulse interval for a simulation with a group of 10 bats (A-C) and how echo detection was determined (D-F). A-E show the full interpulse interval of 100 ms, while F shows an enlargement of the first 10 ms.

A) Timing and received SPL of the individual echoes reflected off neighbors. The echoes arrive at delays corresponding to the neighbors' distance from the focal bat. The vertical lines single out one specific target echo to illustrate the simulated auditory system (see F).

B) Timing and received SPL of the calls from neighboring bats arriving randomly with a uniform probability over the interpulse interval.

C) Timing and received SPL of the secondary echoes in the interpulse interval, arriving randomly with uniform probability over the interpulse interval.

D) The masker SPL profile obtained by adding the effective masker SPL of all maskers (calls and secondary echoes) over time for the chosen echo. The effective masker SPL is the received SPL corrected for spatial unmasking based on the angular separation between the echo and the masker, using the spatial unmasking function in Fig. S2.

E) The echo-to-masker ratio profile obtained by normalizing the echo SPL to the masker SPL profile. 0 dB is the echo's relative SPL.

F) Determining whether an echo was heard or not, by comparing the echo-to-masker ratio profile (solid green) to the temporal masking envelope (dashed pink). If the echo-to-masker ratio is above the temporal masking envelope, then the echo was not masked. In contrast, if the echo-to-masker ratio is cumulatively below the temporal masking envelope for more than 25% of the echo's duration (of 1 or 2.5 ms), then the echo was considered masked. The vertical lines indicate the actual temporal location of the example echo from A). The temporal masking envelope is centered on the chosen echo. Here, the echo-to-masker ratio is below the temporal masking envelope for almost a whole echo duration, meaning that this echo was masked.

6. Supplementary References

1. Sümer S, Denzinger A, Schnitzler H-U (2009) Spatial unmasking in the echolocating Big Brown Bat, *Eptesicus fuscus*. *J Comp Physiol A* 195(5):463–472.
2. Rohatgi A (2015) WebPlotDigitizer. Available at: <https://automeris.io/WebPlotDigitizer/>.
3. Jakobsen L, Surlykke A (2010) Vespertilionid bats control the width of their biosonar sound beam dynamically during prey pursuit. *Proc Natl Acad Sci* 107(31):13930–13935.
4. Jakobsen L, Ratcliffe JM, Surlykke A (2013) Convergent acoustic field of view in echolocating bats. *Nature* 493(7430):93–96.
5. Surlykke A, Pedersen SB, Jakobsen L (2012) Echolocating bats emit a highly directional sonar sound beam in the field. *Proc R Soc B Biol Sci* 276(1658):853–860.
6. Giuggioli L, McKetterick TJ, Holderied M (2015) Delayed Response and Biosonar Perception Explain Movement Coordination in Trawling Bats. *PLoS Comput Biol* 11(3):1–21.
7. Stidsholt L, et al. (2018) A 2.6-g sound and movement tag for studying the acoustic scene and kinematics of echolocating bats. *Methods Ecol Evol* (October):1–11.
8. Firzlaff U, Schuller G (2003) Spectral directionality of the external ear of the lesser spear-nosed bat, *Phyllostomus discolor*. *Hear Res* 185(1–2):110–122.
9. De Mey F, Reijniers J, Peremans H, Otani M, Firzlaff U (2008) Simulated head related transfer function of the phyllostomid bat *Phyllostomus discolor*. *J Acoust Soc Am* 124(4):2123–2132.
10. Goerlitz HR (2018) Weather conditions determine attenuation and speed of sound : Environmental limitations for monitoring and analyzing bat echolocation. *Ecol Evol* 8(March):5090–5100.
11. Lawrence BD, Simmons JA (1982) Measurements of atmospheric

- attenuation at ultrasonic frequencies and the significance for echolocation by bats. *J Acoust Soc Am* 71(3):585–590.
12. Speaks CE (1996) *Introduction to Sound: Acoustics for the Hearing and Speech Sciences* (Singular Publishing Group, Inc., San Diego, California). Second.
 13. Bridson R (2007) Fast Poisson disk sampling in arbitrary dimensions. *ACM SIGGRAPH 2007 sketches - SIGGRAPH '07*:22-es.
 14. Theriault DH, et al. (2010) Reconstruction and Analysis of 3D Trajectories of Brazilian Free-tailed Bats in Flight. *Bost Univ Comput Sci Technical Rep* (Figure 2):1–7.
 15. Wisniewska DM, et al. (2015) Range-dependent flexibility in the acoustic field of view of echolocating porpoises (*Phocoena phocoena*): Short title: Flexible field of view in echolocating porpoises. *Elife* 2015(4):1–29.
 16. Bullock TH, Hopkins CD, Popper AN, Fay RR eds. (2005) *Electroreception* (2005 Springer Science+Business Media, Inc, New York).
 17. Ghose K (2006) Steering by Hearing: A Bat's Acoustic Gaze Is Linked to Its Flight Motor Output by a Delayed, Adaptive Linear Law. *J Neurosci* 26(6):1704–1710.
 18. Lee WJ, et al. (2017) Tongue-driven sonar beam steering by a lingual-echolocating fruit bat. *PLoS Biol* 15(12):1–15.
 19. Richards MA, Scheer J., Holm WA (2010) *Principles of Modern Radar* (SciTech Publishing, Edison, New Jersey).
 20. Cook JC (1985) Target Strength and Echo Structure. *Adaptive Methods in Underwater Acoustics*, ed Urban HG (D. Reidel Publishing Company), pp 155–172.
 21. Götze S, Koblitz JC, Denzinger A, Schnitzler HU (2016) No evidence for spectral jamming avoidance in echolocation behavior of foraging pipistrelle bats. *Sci Rep* 6(July):1–13.
 22. Yost WA (2007) *Fundamentals of hearing: an introduction* (Academic Press, London).
 23. Hase K, et al. (2018) Bats enhance their call identities to solve the cocktail

- party problem. *Commun Biol* 1(1):39.
24. Oliphant TE (2006) *A guide to NumPy* (Trelgol Publishing USA).
 25. Virtanen P, et al. (2019) SciPy 1.0--Fundamental Algorithms for Scientific Computing in Python. *arXiv Prepr*:1–22.
 26. McKinney W (2010) Data Structures for Statistical Computing in Python. *Proc 9th Python Sci Conf (SciPy 2010)*.
 27. Hunter JD (2007) Matplotlib: A 2D graphics environment. *Comput Sci Eng* 9(3):90–95.
 28. Seabold S, Perktold J (2010) Econometric and statistical modeling with Python. *Proc 9th Python Sci Conf (SciPy 2010)*.
 29. Geier M (2015) sounddevice 0.3.5. Available at: https://python-sounddevice.readthedocs.io/en/0.3.5/_modules/sounddevice.html.
 30. Anaconda (2016) Anaconda Software Distribution, Vers 2-2.4.0, Nov. 2016, <https://anaconda.com>.
 31. Van Rossum G (1991) Interactively Testing Remote Servers Using the Python Programming Language. *CWI Q* 4(December):283–303.
 32. Siewert I, Schillinger T, Schmidt S (2004) Forward masking and its consequences for echo perception in the gleaning bat, *Megaderma lyra* (Echolocation in bats and dolphins. University of Chicago Press, Chicago).